Uncertainties in ECMWF Surface Pressure Fields over the Ocean in Relation to Sea Level Analysis and Modeling

RUI M. PONTE

Atmospheric and Environmental Research, Inc., Lexington, Massachusetts

JOEL DORANDEU

CLS Space Oceanography Division, Toulouse, France

(Manuscript received 8 March 2002, in final form 24 July 2002)

ABSTRACT

Knowledge of atmospheric surface pressure (P_a) over the oceans is important for proper interpretation and modeling of sea level variability. Gridded analyses of P_a fields from the European Centre for Medium-Range Weather Forecasts (ECMWF) have been routinely used for altimeter data processing, but their uncertainties are poorly understood. An attempt is made here to quantify the uncertainties in ECMWF P_a fields over the period 1993–95, coinciding with the early years of the TOPEX/Poseidon altimeter mission, by using similar fields from a different operational analysis, a limited set of island barometer records, and TOPEX/Poseidon sea level data. The analysis presented here suggests that ECMWF error variances are under 3 hPa^2 over most of the oceans, with typical values closer to 1 hPa^2 or smaller, but with substantially larger errors south of 50°S. The worst signal-to-noise ratios occur in the Tropics, where P_a variance is smallest. Errors are mostly associated with uncertainties in submonthly P_a signals.

1. Introduction

Atmospheric surface pressure P_a is an important variable in the study of ocean surface variability, particularly sea level ζ. At sufficiently low frequencies, P_a drives a static or so-called inverted barometer (IB) response in the ocean, which entails adjustments in ζ at a rate of approximately -1 cm hPa^{-1}. At subweekly periods, dynamic effects become important. For both regimes, fluctuations in P_a can be more important than winds in accounting for observed ζ signals (Ponte 1994; Tierney et al. 2000). Besides directly driving ζ variability, P_a also affects retrieval of ζ estimates from altimeter measurements through its effects on the dry-tropospheric and sea-state bias corrections (e.g., Chelton et al. 2001).

For IB regimes, an error of 1 hPa in P_a estimates translates into an error of 1 cm in ζ (if over 100 km, this corresponds to 1 cm s^{-1} error in geostrophic surface current estimates at midlatitudes). At rapid (daily) timescales, errors in P_a can be amplified given the dynamic, resonant nature of the response (Ponte 1993). Our ability to interpret and model ζ and surface current variability thus clearly depends on how well we can determine P_a. Given the very sparse directly observed data over the oceans, one has to rely on gridded P_a fields produced by various weather centers. The analyzed fields are of course not perfect, but it is difficult to quantify their uncertainties. The topic is an active area of investigation at the weather centers but error estimates, in particular for the analyzed P_a fields of interest, are not an easy find in the literature.

With the increasing needs for accurate determination of ζ—1-cm accuracy is the goal for the new *Jason-1* altimeter mission—and with modeling of P_a-driven signals becoming more and more important (Hirose et al. 2001), quantitative estimates of errors in available P_a fields seem warranted. Pressure fields from the European Centre for Medium-Range Weather Forecasts (ECMWF) have been routinely used for TOPEX/Poseidon (T/P) data processing since late 1992. In this paper, we try to assess the errors in ECMWF P_a analysis during the first years of the T/P mission by comparing ECMWF fields with a limited number of island stations and with another widely used product, namely, that of the National Centers for Environmental Prediction (NCEP). The datasets and methodology are introduced in section 2 and inferences on error variances of ECMWF P_a fields are drawn in section 3. A summary of results and final remarks are provided in section 4.

Corresponding author address: Dr. Rui M. Ponte, Atmospheric and Environmental Research, Inc., 131 Hartwell Ave., Lexington, MA 02421-3126.
E-mail: ponte@aer.com

TABLE 1. Island stations, location, number of days in the records, and respective variances including estimates from ECMWF and NCEP.

Station	Lat (°N)	Lon (°E)	No. of days	Variance (hPa^2)		
				Data	ECMWF	NCEP
Adak	51.87	183.37	1037	197.8	196.7	198.1
Bermuda	32.37	295.31	920	30.6	29.8	30.3
Cocos	−12.12	96.90	588	4.5	4.6	4.6
Diego Garcia	−7.29	72.39	1002	4.0	3.7	4.6
Diego Ramirez	−56.51	291.29	970	133.2	128.3	140.9
Easter	−27.15	250.55	968	23.3	22.1	22.4
Guam	13.44	144.65	1017	5.2	5.2	5.9
Honolulu	21.3	202.13	1033	6.3	6.2	6.2
Kwajalein	8.74	167.74	1034	2.6	3.0	3.0
Midway	28.21	182.64	1051	23.2	23.6	24.1
Pago Pago	−14.28	189.32	1033	6.5	5.3	5.4
Praia	14.91	336.49	452	3.5	3.4	4.9
São Miguel	37.74	334.33	863	57.9	57.5	58.6
Socorro	18.71	249.05	1031	7.0	7.3	6.2
Wake	19.29	166.62	1049	5.4	5.7	5.8

2. Data and methodology

Sea level P_a fields from ECMWF and NCEP operational products for a 3-yr period (1993–95) were retrieved from the archives at the National Center for Atmospheric Research. The particular years chosen overlap with the T/P mission and have been studied extensively in that context. We note, however, that the operational products are continuously evolving with the implementation of changes in atmospheric models and data assimilation schemes. Thus, our results only apply strictly to the period of study.

Both ECMWF and NCEP are 6-hourly products given at the same times and on Gaussian grids in latitude and regular grids in longitude but with different spacing: 160 (190) points in latitude and 1.125° (0.9375°) in longitude for ECMWF (NCEP). The ECMWF fields were interpolated in latitude to a regular 1.125° grid. The NCEP fields were bilinearly interpolated to the slightly coarser 1.125° × 1.125° ECMWF grid. The interpolation adds some uncertainty to the NCEP fields and thus favors the ECMWF analysis, but is consistent with our focus on the latter. A number of time samplings (100 points altogether) were missing in the NCEP fields. These dates were flagged and not used in our analysis. In addition, preliminary comparisons of the two time series revealed a time offset of 6 h between them. The difference was traced to the fact that the archived NCEP P_a values were actually 6-h forecasts. (For simplicity we will refer to both ECMWF and NCEP fields as analyses, but this difference should be kept in mind.) The original NCEP times were thus shifted by 6 h, to correct for the time tag problem.

To compare with the analyses, we obtained a number of island station pressure data that were available online at a site maintained by the National Oceanic and Atmospheric Administration/National Ocean Service's (NOAA/NOS) Center for Operational Oceanographic Products and Services (http://co-ops.nos.noaa.gov/). The 15 stations used (see Table 1) correspond to a subset of those used by Ray (1998) in a study of atmospheric tides. Although the spatial coverage is limited, it spans both low and high latitudes. The hourly time series at each island were checked for missing values and outliers and subsampled at the times of the analyses. Most series cover nearly the whole 3-yr period (1993–95), with the exception of Praia and Cocos, which have less than 2 yr of data (Table 1). For the comparisons with the island data, ECMWF and NCEP fields were bilinearly interpolated to each station location.

Analyses of T/P data consist in estimating the impact of IB corrections based on different P_a fields on the observed sea surface height (SSH) variance. The IB correction is essentially proportional to $P_a - \overline{P}_a$, where $\overline{P}_a$ is the average P_a over the ocean (Ponte 1993). The latest SSH data distributed by Archiving, Validation and Interpretation of Satellite Oceanographic Data (AVISO) group Merged Geophysical Data Record, version C are used after applying the usual editing criteria (Le Traon et al. 1994) and altimetric corrections. SSH differences at crossover points are computed for the period 1993–95. Only crossover differences with a time lag lower than 10 days are selected, to focus on high frequencies at which, as we shall see, most of the differences in P_a fields are found and to avoid effects of contamination by longer-period ocean signals not related to P_a. For the IB correction based on ECMWF or NCEP fields, the instantaneous pressure value is obtained by interpolating the gridded values to the specific time and location of the altimeter measurements, and $\overline{P}_a$ is allowed to vary in time and computed every 6 h.

3. Assessing errors in ECMWF fields

We seek approximate estimates of the uncertainties in the gridded ECMWF P_a fields over the ocean. Our approach is to compare ECMWF fields with those of NCEP and to infer a measure of the combined error variances in both analyses, and then use the island re-

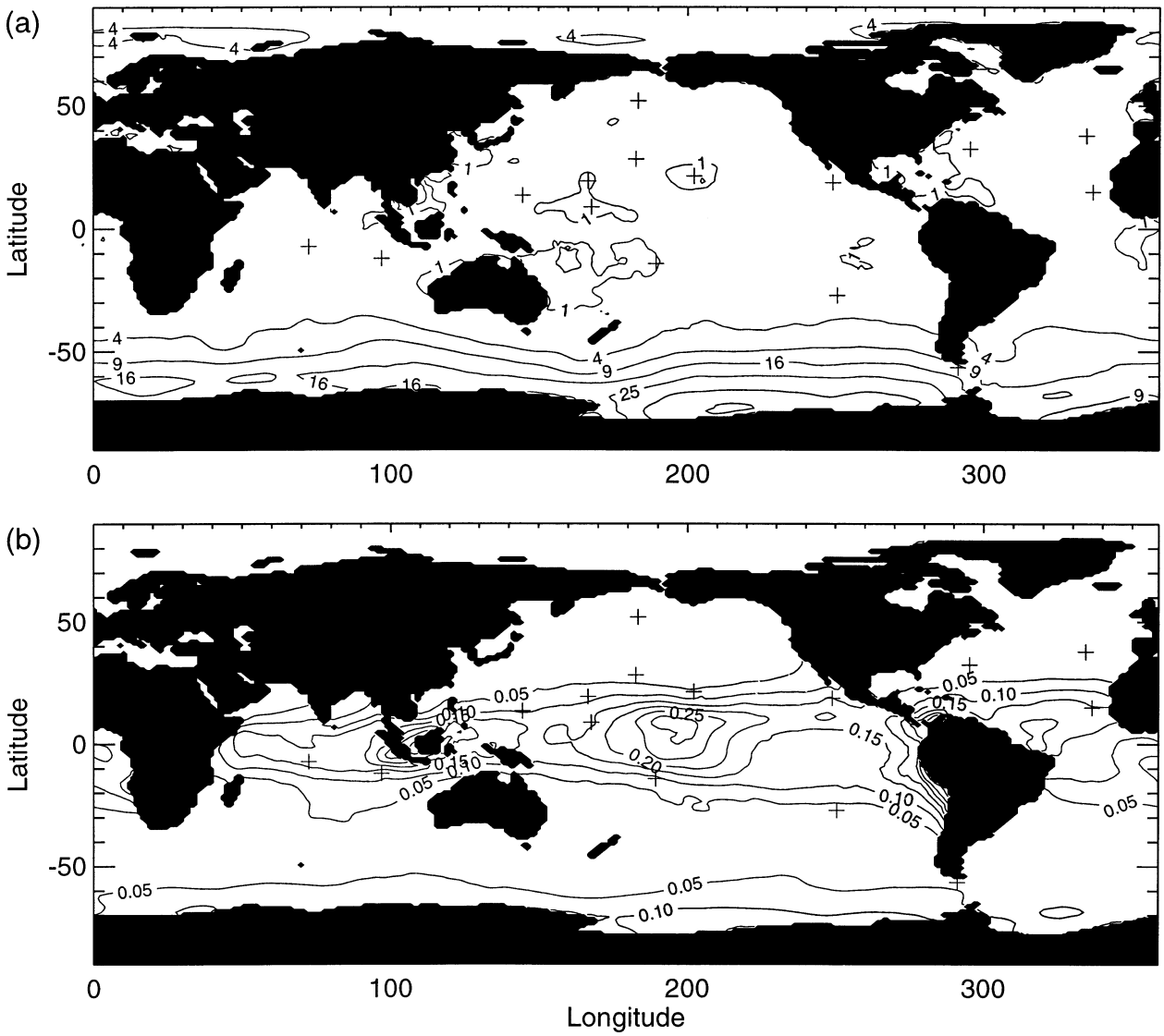

FIG. 1. (a) Values of $\langle (N - E)^2 \rangle$ (in hPa^2), where N and E are pressure values for NCEP and ECMWF, respectively. Contour interval is n^2 with $n = 1, 2, 3, \ldots$, for ease of comparison with Fig. 25 of Chelton et al. (2001). (b) Ratio of $\langle (N - E)^2 \rangle$ to $\langle N^2 \rangle + \langle E^2 \rangle$. Contour interval is 0.05. Crosses are drawn at the locations of the pressure station data used in Table 1.

cords and T/P data to assess how these errors may be partitioned between the analyses.

a. Comparison of analyses

Differences between two P_a fields indicate errors in at least one of the series. Letting each record represent the true signal plus noise, then

$$\langle (N - E)^2 \rangle = \langle N'^2 \rangle + \langle E'^2 \rangle - 2\langle N'E' \rangle, \qquad (1)$$

where we use N and E to denote P_a fields from NCEP and ECMWF, respectively, and prime quantities represent errors. For weakly correlated errors, $\langle (N - E)^2 \rangle$ represents the sum of the error variances in both analyses. Some degree of positive correlation between N' and E' is expected, however, given that these analyses share common data and model features (see section 3b). Thus, $\langle (N - E)^2 \rangle$ can be taken to represent a lower bound on the value of $\langle N'^2 \rangle + \langle E'^2 \rangle$. Values of $\langle (N - E)^2 \rangle$ are shown in Fig. 1a. We focus on the time variability and thus have subtracted the local means from both fields (mean bias between the two centers is ~0.5 hPa).

Variances in Fig. 1a range from <4 hPa^2 over most of the ocean to substantially larger values over the Southern Ocean, particularly in the Pacific sector. The sharp poleward increase in the Southern Hemisphere is not seen in the Northern Hemisphere and thus is not simply due to the well-known poleward increase in P_a variance (e.g., Ponte 1993) but more likely related to

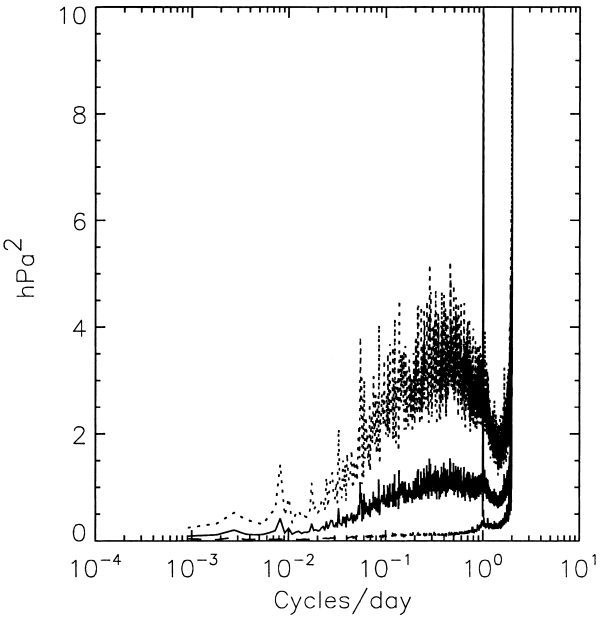

FIG. 2. Frequency times spectral values of $N - E$ time series averaged over the whole ocean (solid), the Southern Ocean (dotted), and the tropical ocean (dashed). The variance contributed by any frequency band is proportional to the respective area under the curve.

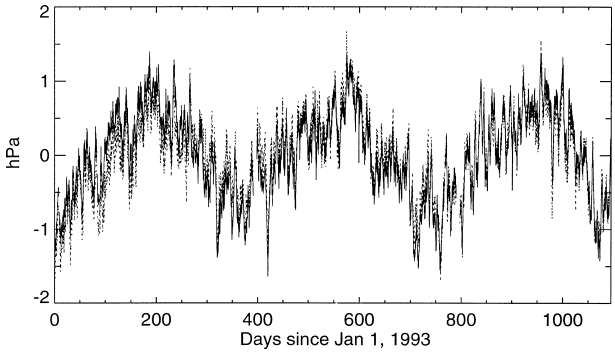

FIG. 3. Time series of $\overline{P}_a$ for ECMWF (solid) and NCEP (dotted). Curves are not drawn at times for which NCEP values are not available.

the much sparser data coverage and the degraded quality of the analyses expected in those regions. Large discrepancies in surface pressure analysis over the Southern Ocean have been noted (vanDam and Wahr 1993). Results in Fig. 1a can also be compared with similar quantities shown by Chelton et al. (2001, their Fig. 25) but based on the period 1993–97. Our values indicate somewhat smaller differences between NCEP and ECMWF analyses. Differences calculated without accounting for NCEP 6-h shift mentioned in section 2 did produce values and patterns much more similar to those of Chelton et al. Thus, their results are probably affected by the time alignment problem.

The ratio of $\langle (N - E)^2 \rangle$ to the variance $\langle N^2 \rangle + \langle E^2 \rangle$ (Fig. 1b) gives a measure of how well determined the P_a signals are on average in both analyses. High southern latitudes show error variances between 5% and 15% of the estimated variances. For most other regions outside the Tropics, the above ratio is at most 5%. Values of P_a in the Tropics are comparatively more noisy, in part because the signal variance is also small. The semidiurnal atmospheric tide contributes substantially to the P_a variance in the Tropics. The largest ratios in Fig. 1b tend to occur at tropical longitudes where the 6-h analyses always sample the semidiurnal tide near its nodes (e.g., Van den Dool et al. 1997), thus underestimating the P_a variability.

Spectral analysis of $N - E$ time series can be used to check the expected distribution of error variance with frequency. To have continuous series for calculating the spectra, values of $N - E$ were set to zero where gaps in the NCEP series occur. Spectra were calculated every four grid points and then averaged globally to yield the variance preserving spectra in Fig. 2. There are large peaks at diurnal and semidiurnal periods, which reflect the uncertainties in the estimates of the atmospheric tides. Maxima in the synoptic band (~1–10 days) are also particularly clear in the spectrum for the Southern Ocean. In general, submonthly periods contribute dominantly to the variance in Fig. 1a. The median period for the globally averaged spectrum is 3.6 days but drops to 1 day in the Tropics where diurnal and semidiurnal harmonics alone account for ~14% of the variance.

For purposes of ζ and IB analysis, it is also relevant to assess uncertainties in $\overline{P}_a$, the average of P_a over the oceans. Time dependence of $\overline{P}_a$ is particularly important in the analysis of tropical data (Ponte 1993; Dorandeu and Le Traon 1999), but uncertainties in $\overline{P}_a$ are unknown. Time series of $\overline{P}_a$ based on ECMWF and NCEP fields (Fig. 3) have variances of 0.34 and 0.31 hPa^2, respectively, similar to the estimates of Ponte (1993) and Wunsch and Stammer (1997). The curves are fairly coherent on all timescales, but there are noticeable discrepancies at times. With a mean bias of 0.2 hPa removed, the mean-square difference of the two curves is ~0.05 hPa^2, suggesting error variances <10% of the estimated variance in $\overline{P}_a$ and substantially smaller than the error variances in P_a.

b. Comparisons with island data

Without extra information or data, it is difficult to determine how the errors implicit in Figs. 1a and 2 are partitioned between analyses. In addition, one has the ambiguity related to the unknown term $\langle N'E' \rangle$. We attempt to get at the problem by using the island barometers to estimate all the terms in (1) at a few locations. Extrapolation of results from these sites to other regions is not a given, but this approach provides at least some guidance on how to interpret results in section 3a. Instrument error is taken to be negligible. Barometer readings are reported to within 0.1 hPa, which is the specified instrument noise (e.g., Dai and Wang 1999) barring

TABLE 2. Variances and covariance of $E - D$ and $N - D$ (units: hPa^2).

Station	$\langle(E - D)^2\rangle$	$\langle(N - D)^2\rangle$	$\langle(E - D)(N - D)\rangle$
Adak	1.21	2.63	0.77
Bermuda	0.65	1.31	0.37
Cocos	0.25	1.08	0.17
Diego Garcia	0.53	1.61	0.39
Diego Ramirez	2.83	10.96	2.02
Easter	0.43	1.44	0.19
Guam	0.24	1.04	0.13
Honolulu	0.14	0.83	0.12
Kwajalein	0.22	0.83	0.11
Midway	0.71	1.32	0.34
Pago Pago	0.50	1.34	0.45
Praia	0.27	1.10	0.06
São Miguel	0.28	1.19	0.19
Socorro	1.31	1.74	0.53
Wake	0.22	0.88	0.09

any clear malfunctions of the instruments. Many island P_a observations, including possibly some of the records examined here, are assimilated routinely at both ECMWF and NCEP, but the analyses are only allowed to fit the data within expected representation errors (i.e., errors due to processes or scales present in the data that cannot be represented by the model used in the analyses). Thus, differences between analyses and island records examined here can be interpreted as a measure of representation errors in the analyses, approximating the true error made when using gridded P_a fields in ζ analysis at a point.

Table 1 displays the variance of each island record together with respective ECMWF and NCEP values. Variances range from a few hectopascals squared at low latitudes to more than 100 hPa^2 at high latitudes. The estimated variances in both analyses match very well the observed variances: differences are $\sim$1 hPa^2 or smaller, with the exception of Diego Ramirez, Chile, for which NCEP shows $\sim$7 hPa^2 more variance and ECMWF $\sim$5 hPa^2 less variance than the data. The island of Diego Ramirez is located near the tip of South America and the larger discrepancies are consistent with the indication from Fig. 1a of larger analysis errors in those regions.

A simple measure of fit between analyses A and data D is given by their mean-square differences:

$$\langle(A - D)^2\rangle = \langle A'^2\rangle + \langle D'^2\rangle - 2\langle A'D'\rangle, \qquad (2)$$

where again prime quantities represent errors. For negligible instrument errors D', terms $\langle D'^2\rangle$ and $\langle A'D'\rangle$ can be ignored and the mean-square differences represent the error variance in the analysis. Estimates of (2) for ECMWF and NCEP analyses (Table 2) range between 0.1 and 11 hPa^2, indeed much larger than the expected value of $\langle D'^2\rangle \sim$ (0.1 hPa)^2, given the mentioned uncertainties in barometer readings.

Mean-square differences between ECMWF and station records are mostly $\sim$1 hPa^2 or smaller, with the exception of Diego Ramirez (2.83 hPa^2) where observed variance is also large (Table 1). Agreement is thus surprisingly good even at Diego Ramirez. When compared to NCEP, ECMWF series are closer to the data at all stations. Mean-square differences for NCEP are typically 2–4 times larger than those of ECMWF ($\sim$6 times at Honolulu).

The island data can also be used to gain information on the term $\langle N'E'\rangle$ in (1). For negligible data error one has

$$\langle(E - D)(N - D)\rangle = \langle E'N'\rangle + \langle D'^2\rangle - \langle E'D'\rangle - \langle N'D'\rangle \approx \langle E'N'\rangle. \qquad (3)$$

Estimates of the covariance $\langle(E - D)(N - D)\rangle$ given in Table 2 yield positive values at all stations, indicating the presence of positively correlated errors in the analyses. Amplitudes of $\langle E'N'\rangle$ based on (3) are not negligible compared to the estimated error variances ($\langle(E - D)^2\rangle$ and $\langle(N - D)^2\rangle$ columns in Table 2). As inferred from Table 2, values of $\langle(E - N)^2\rangle$ can be lower than the sum of the error variances $\langle E'^2\rangle + \langle N'^2\rangle$ by as much as $\sim$50% (Pago Pago), with the average bias being $\sim$30%.

In summary, based on the comparisons with island data, values of $\langle(E - N)^2\rangle$ in Fig. 1a can underestimate the value of $\langle N'^2\rangle + \langle E'^2\rangle$ by as much as 50% because of positive error correlations. While the values in Fig. 1a give a lower bound on $\langle N'^2\rangle + \langle E'^2\rangle$, doubling those values might provide a plausible upper bound. In addition, from the typical 2–4 ratios of NCEP to ECMWF error variances inferred from Table 2, errors in ECMWF P_a fields may amount to between 1/3 and 1/5 of the estimated $\langle N'^2\rangle + \langle E'^2\rangle$ values. Whether these conclusions based on island records can be extrapolated in general to other places is difficult to assert, but useful insight can be gained from the analysis of the global and independent T/P data.

c. Comparisons with sea level data

The IB corrections based on the two different P_a fields are applied to the T/P SSH crossover differences. The variances of the corrected crossover sets are then compared to yield a measure of the relative performances of the NCEP- and ECMWF-based IB corrections. Differences in SSH crossover variance for the NCEP and ECMWF cases, calculated over each 10-day cycle for the period 1993–95, are shown in Fig. 4. The results are expressed as a percentage of the crossover variance in the ECMWF-corrected set. Positive values obtained for most of the cycles shown indicate that the ECMWF correction is generally better, judging by the smaller variance in the SSH variability. The ECMWF correction leads to crossover variances $\sim$5% or 3.6 cm^2 smaller on average than those obtained with the NCEP correction. (If caused by P_a errors alone, the difference in

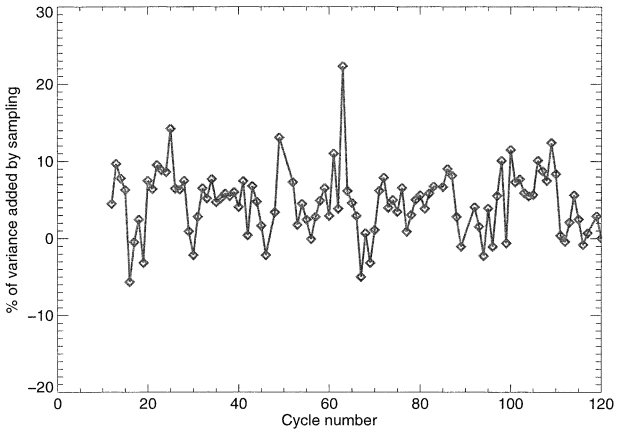

FIG. 4. Difference in crossover variance after applying IB corrections based on NCEP and ECMWF fields over each T/P cycle, expressed as a percentage of the crossover variance after ECMWF-based correction is applied. Positive values imply better performance of ECMWF fields. Cycles 50, 51, 90, and 91 are not shown, as they coincide with periods with a substantial number of missing NCEP values.

crossover variances would imply a mean difference of ~3.6 hPa^2 in ECMWF and NCEP error variances.)

The relative performances of the two IB corrections are geographically analyzed in Fig. 5. For the whole 1993–95 period, the crossover variances are calculated in 4° bins, and the differences between NCEP- and ECMWF-corrected values are computed. Results show that the ECMWF fields produce much smaller crossover variances particularly at southern high latitudes (red bins). More than 4 cm^2 of excess variance relative to ECMWF is found poleward of 50°S. Elsewhere the results are more balanced, but the zones where the NCEP correction produces lower SSH variance (blue bins) are very few. The T/P analysis thus supports the assertion that the smaller errors in ECMWF fields inferred from the island comparisons can be generalized to most regions and in particular to those regions with largest P_a errors.

4. Summary and final remarks

Conservatively taking $\langle E'^2\rangle/\langle N'^2\rangle \sim 1/2$, then from results in Fig. 1a, values of $\langle E'^2\rangle$ can range from <1 hPa^2 over most of the oceans to >3 hPa^2 at most latitudes south of 50°S (largest values >12 hPa^2 in the Pacific sector of the Southern Ocean). Comparison with island barometers suggests that errors in analyzed fields are positively correlated, consistent with other studies (e.g., Gaspar and Ponte 1997). If one considers those effects, doubling the above values provides a plausible upper bound on $\langle E'^2\rangle$. Errors are estimated to be at least twice as large for NCEP. Note, however, that the NCEP fields used here are interpolated to the ECMWF grid and are based on 6-h forecasts, which may partly explain the larger errors. Better judgment of NCEP P_a errors should await calculations using analyzed fields.

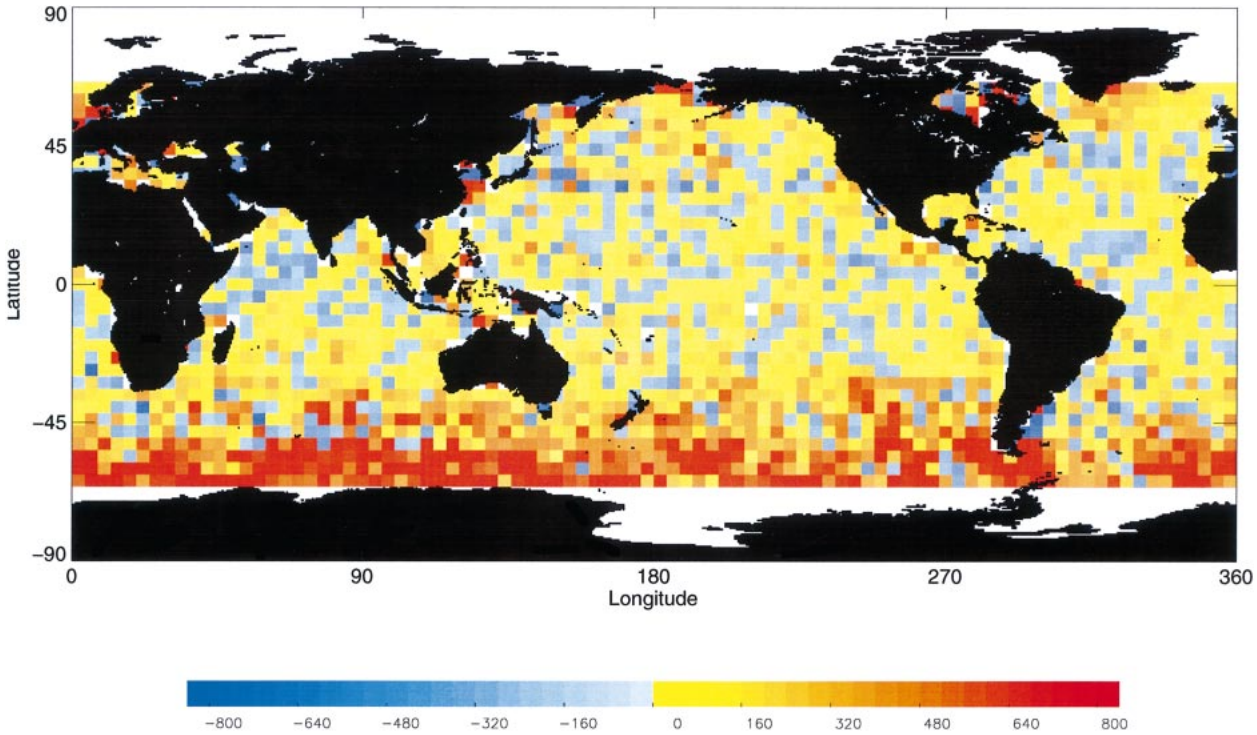

FIG. 5. Difference in crossover variance (mm^2) for IB-corrected data based on NCEP and ECMWF fields over the period 1993–95. Positive values indicate larger variance reduction obtained with an ECMWF-based IB correction.

Our findings suggest that most of the P_a errors are associated with submonthly variability and that their spatial structure is likely not zonally homogeneous or symmetric about the equator. Error models that assume statistics independent of longitude and are hemispherically symmetric might be relaxed to account for some of the patterns observed in Fig. 1a. Some P_a error models do allow for variable statistics by assuming a linear relation between error and estimated P_a variance (e.g., Gaspar and Ponte 1997). The results for our period of study indicate that these linear models should allow for smaller signal-to-noise ratios likely present in regions such as the Tropics and high southern latitudes, as inferred from Fig. 1b.

Combining in situ and satellite data with different gridded P_a products can yield useful quantitative information on the error variances of the latter and, although not pursued here, also on their time and spatial covariances. Our attempt was limited by the small amount of P_a data examined. The use of the T/P altimeter essentially as a global barometer can be helpful, but SSH measurements are not a direct measure of P_a and their accuracy is not comparable to true barometer readings. An alternative for future studies is to use a more comprehensive set of island barometers and also data from ships (e.g., Smith et al. 2001) and buoys.

Finally, we emphasize again that our results strictly apply only to the period of study. As models, data collection, and assimilation schemes evolve with time, the quality of the analyses should improve. One example of a change that might have a positive impact on the estimation of P_a fields is the recent start of routine assimilation of scatterometer wind data at ECMWF and NCEP. It would be useful to pursue studies of the sort performed here for more recent years, using an extended set of in situ data and P_a products, in order to better quantify uncertainties in each available P_a field and, if possible, determine which are the best ones for ζ analysis and modeling.

Acknowledgments. We thank P. Nelson for help with the initial processing of the pressure fields and R. Ray for pointing us to the island data. Support for this work at AER was provided by the NASA *Jason-1* project under Contract 1206432 with the Jet Propulsion Laboratory. Pressure fields comparisons at altimeter crossovers carried out at CLS were funded by CNES.

REFERENCES

Chelton, D. B., J. C. Ries, B. J. Haines, L.-L. Fu, and P. S. Callahan, 2001: Satellite altimetry. *Satellite Altimetry and Earth Sciences*, L.-L. Fu and A. Cazenave, Eds., Academic Press, 1–131.

Dai, A., and J. Wang, 1999: Diurnal and semidiurnal tides in global surface pressure data. *J. Atmos. Sci.,* **56,** 3874–3891.

Dorandeu, J., and P.-Y. Le Traon, 1999: Effects of global mean atmospheric pressure variations on mean sea level changes from TOPEX/Poseidon. *J. Atmos. Oceanic Technol.,* **16,** 1279–1283.

Gaspar, P., and R. M. Ponte, 1997: Relation between sea level and barometric pressure determined from altimeter data and model simulations. *J. Geophys. Res.,* **102,** 961–971.

Hirose, N., I. Fukumori, V. Zlotnicki, and R. M. Ponte, 2001: High-frequency barotropic response to atmospheric disturbances: Sensitivity to forcing, topography, and friction. *J. Geophys. Res.,* **106,** 30 987–30 996.

Le Traon, P.-Y., J. Stum, J. Dorandeu, P. Gaspar, and P. Vincent, 1994: Global statistical analysis of TOPEX and POSEIDON data. *J. Geophys. Res.,* **99,** 24 619–24 631.

Ponte, R. M., 1993: Variability in a homogeneous global ocean forced by barometric pressure. *Dyn. Atmos. Oceans,* **18,** 209–234.

——, 1994: Understanding the relation between wind- and pressure-driven sea level variability. *J. Geophys. Res.,* **99,** 8033–8039.

Ray, R., 1998: Diurnal oscillations in atmospheric pressure at twenty-five small oceanic islands. *Geophys. Res. Lett.,* **25,** 3851–3854.

Smith, S. R., D. M. Legler, and K. V. Verzone, 2001: Quantifying uncertainties in NCEP reanalyses using high-quality research vessel observations. *J. Climate,* **14,** 4062–4072.

Tierney, C., J. Wahr, F. Bryan, and V. Zlotnicki, 2000: Short-period oceanic circulation: Implications for satellite altimetry. *Geophys. Res. Lett.,* **27,** 1255–1258.

van Dam, T. M., and J. Wahr, 1993: The atmospheric load response of the ocean determined using Geosat altimeter data. *Geophys. J. Int.,* **113,** 1–16.

Van den Dool, H. M., S. Saha, J. Schemm, and J. Huang, 1997: A temporal interpolation method to obtain hourly atmospheric surface pressure tides in reanalysis 1979–1995. *J. Geophys. Res.,* **102,** 22 013–22 024.

Wunsch, C., and D. Stammer, 1997: Atmospheric loading and the oceanic ''inverted barometer'' effect. *Rev. Geophys.,* **35,** 79–107.